Rate Constants for the Gas-Phase Reactions of Silylene with Methanol, Deuterated Methanol, and Water

Ula N. Alexander,[†] Keith D. King,*[,‡] and Warren D. Lawrance[†]

School of Chemistry, Physics and Earth Sciences, Flinders University, GPO Box 2100, Adelaide SA 5001, Australia, and Department of Chemical Engineering, Adelaide University, Adelaide SA 5005, Australia

Received: July 18, 2001; In Final Form: October 31, 2001

Gas-phase reaction rate constants for the reaction of silylene, SiH_2, with deuterated methanol, CD_3OD, have been determined over the temperature range 294−423 K and at total pressures over the range 100−800 Torr of the inert bath gas, Ar. Rate constants have also been measured for the reaction of SiH_2 with CH_3OH at 294 K over the range 100−800 Torr, also with Ar. Rate constants for the reaction of SiH_2 with H_2O over the range 50−200 Torr in Ar have been determined at 294 K. The second-order rate constants are pressure-dependent up to the maximum pressures investigated. For CD_3OD, for which temperature-dependent data have been obtained, the rate constants decrease with increasing temperature, indicating that the reaction proceeds via the formation of a complex. At the highest temperature studied (423 K), the experimental decay curves indicate the system approaching equilibrium, providing direct experimental evidence for the formation of the complex. Analysis of the 423 K decay curves provides an experimental determination of the equilibrium constant, K_{eq}, and a value for the dissociation energy of the complex of 83.0 ± 1.3 kJ mol^{-1}. The Rice−Ramsperger−Kassel−Marcus (RRKM)/master equation modeling gives a dissociation energy for the SiH_2−CD_3OD complex of 83.7 kJ mol^{-1}. Ab initio calculations, performed at the MP2/6-311+G** level of theory, give a value of 75.4 kJ mol^{-1}, in reasonable agreement with this value. The RRKM/master equation modeling for SiH_2 + CD_3OD, when adjusted to account for the changes arising from deuteration, reproduces the behavior observed for SiH_2 + CH_3OH. The high-pressure limit predictions of the RRKM/master equation modeling are quite unusual and may indicate unusual pressure and temperature behavior in weakly bonded systems.

1. Introduction

Silylene, SiH_2, is a reactive intermediate important to a number of industrial processes, the prime example being chemical vapor deposition (CVD) used to deposit silicon films onto substrates during the manufacture of semiconductor components. This has been a major factor driving the interest in SiH_2 kinetics.[1] However, besides the industrial relevance of SiH_2 kinetic studies, there is a desire to understand the fundamental chemistry of the simplest silylene and how its reactions compare to its Group IV analogues, CH_2 and GeH_2.

Prior to 1985, silylenes were studied via indirect methods such as end-product analyses and relative rates.[2−4] Since then, direct time-resolved techniques in the gas phase have allowed more detailed study of the reaction kinetics,[5] including direct insight into reaction intermediates. Gas-phase reactions of dimethylsilylene, $SiMe_2$, have also been studied in some detail using time-resolved techniques.[6−8]

Reviews such as those of Jasinski et al.[9] and Becerra and Walsh[10] provide a summary of the SiH_2 reactions studied. These have involved principally small inorganic molecules, alkanes, alkenes, alkynes, and silanes. It has been found that SiH_2 reacts by insertion into certain types of sigma bonds and by addition across double and triple bonds. Insertion into C−H bonds (alkanes), H−H bonds (hydrogen), and Si−C bonds (substituted silanes) is much slower than insertion into Si−H bonds (silanes) and addition across multiple bonds (alkenes and alkynes). Examples of reactions showing a dependence of the reaction rate on total pressure include SiH_2 reaction with C_2H_4[11] and C_2H_2,[12] which are still pressure-dependent at 100 Torr, the highest pressure accessed experimentally. N_2O and Me_3SiH[10] are notable exceptions to the dependence of the reaction rate on total pressure.

The reactions of SiH_2 with organic analogues of water (e.g., methanol, MeOH, and dimethyl ether, Me_2O) are important to the study of silicone chemistry. They also represent an important class of reactions, namely, SiH_2 with *n*-donor bases. To date, they have received little attention,[10] although Walsh has reported on the reaction of SiH_2 with acetone[13] and, in conjunction with Walsh's group, we have reported the results of a limited study of the reaction of SiH_2 with Me_2O.[14] We have now studied the reaction of SiH_2 with H_2O, MeOH, CD_3OD, and Me_2O in detail with the aim of determining the pressure and temperature dependence of the second-order rate constants for these reactions. These reactants represent a series systematically substituted about the oxygen atom. We have recently reported the results of a detailed study of the temperature and pressure dependence of SiH_2 reaction with Me_2O.[15] The present paper reports results for H_2O, MeOH, and CD_3OD.

The reaction of SiH_2 with these species is expected to occur via the formation of a complex with significant charge-transfer character.[16,17] Our study of Me_2O confirmed the presence of an intermediate complex and provided, through a determination of the equilibrium constant directly from the data at the highest experimental temperature of 441 K, a value for the well depth

* To whom correspondence should be addressed. E-mail: kking@chemeng.adelaide.edu.au.
[†] Flinders University.
[‡] Adelaide University.

10.1021/jp012773v CCC: $22.00
Published on Web 01/16/2002

of the complex.[15] Values for comparison were also determined from ab initio calculations and Rice−Ramsperger−Kassel−Marcus (RRKM)/master equation modeling. In the present work, the same procedures are used to determine the well depth of the complexes. As for the Me_2O case, we find direct experimental evidence for the formation of an intermediate complex for the $SiH_2 + CD_3OD$ reaction through the observation of equilibrium between the reactants and complex at elevated temperatures.

2. Experimental Details

The experimental system is based on that used in our extensive studies of CH_2 ($\tilde{a}\ ^1A_1$) kinetics[18−23] and GeH_2 kinetics.[24,25] The temperature-variable reaction cell has been described previously.[21] Details pertinent to the SiH_2 experiments have been provided in our publication concerning the $SiH_2 + Me_2O$ reaction.[15]

Briefly, $SiH_2(000)$ was generated by 193 nm (ArF) excimer laser photolysis of phenylsilane, $PhSiH_3$, and probed by a single frequency cw laser tuned to the rovibronic transition $^1B_1(020) \leftarrow {}^1A_1(000)\ 5_{05}$ at 17 259.50 cm^{-1} (vac).[26] While 193 nm photolysis of $PhSiH_3$ produces SiH_2 in both the (000) and (010) vibrational states,[27] at total pressures above a few Torr, collision-induced relaxation of vibrationally excited silylene is rapid,[28] and because our experiments are conducted at pressures >50 Torr, vibrational relaxation of the (010) SiH_2 to (000) is not expected to confound our measurements. This was confirmed by testing that the rate constants obtained using 248 nm photolysis, during which much less (010) SiH_2 is produced,[27] were the same as those obtained with 193 nm photolysis. The reactants studied here do not absorb at the photolysis wavelengths of 193 and 248 nm.

The probe laser is split into reference and signal beams that are input to separate channels of a differential amplifier to remove the laser noise from the resultant output. The output of the differential amplifier is averaged over 64−256 photolysis laser shots on a digital oscilloscope, and the resulting trace is transferred to a computer for analysis. To minimize nonsilylene contributions to the signal, two sets of decay traces are recorded: one with the laser tuned to a SiH_2 absorption (signal) and one with the laser detuned from SiH_2 (background). The background is subtracted from the signal to provide the SiH_2 decay signal.

The experiment is performed under conditions such that the reactions are pseudo-first-order and the silylene signal decays exponentially. The CD_3OD study was undertaken at four temperatures from ambient (294 K) to 423 K. With the exception of the highest temperature data, decay traces were fit to a biexponential function to account for both the rise and decay features. The traces did not return to the baseline at the highest temperature. These traces were fitted with a triexponential function having a rise and two decay times. The MeOH and H_2O studies were undertaken at ambient temperature only. The purpose of the MeOH study was to determine the effect of deuteration on the system, and this could be done at a single temperature. In the H_2O case, reaction was so slow that the determination of the rate constants proved very difficult. Absolute minimum amounts of precursor were required to enable the contribution of H_2O to reaction to be differentiated from that of the precursor. Because the reaction rate decreases with increasing temperature, the study of the reaction at elevated temperatures was not feasible with our present apparatus. As for the lower temperature CD_3OD data, the decay traces for MeOH and H_2O showed single-exponential decay and returned to the baseline. They were fit to a biexponential function to account for both the rise and decay features. A minimum of three averaged traces were recorded and analyzed at each reactant pressure.

The rate constants reported here were obtained with total cell pressures of 100−800 Torr for MeOH and CD_3OD and 50−200 Torr for H_2O. Ar was used as the buffer gas. For the MeOH and CD_3OD experiments, the $PhSiH_3$ pressure was typically 10−30 mTorr and the reactant pressure was typically varied in the range 0.5−3.5 Torr. Because the reaction of SiH_2 with H_2O is very slow, for the H_2O experiments it was essential that the minimum pressure of $PhSiH_3$ needed to generate acceptable signal levels be used to minimize the contribution of the precursor to the observed reaction rate of SiH_2. Under our experimental conditions, this corresponds to 3 mTorr of $PhSiH_3$. The low vapor pressure of H_2O, which restricts the upper magnitude of the pseudo-first-order rate constant, compounds the problem. With cell pressures of up to 200 Torr, it was necessary to premix the H_2O with Ar carrier gas to a premix pressure well above the maximum cell pressure. The maximum H_2O partial pressure that could be achieved in the cell was 0.5 Torr. The gases are flowed continuously through the sample cell to prevent the build up of reaction products. Gas flow rates are controlled using mass flow controllers (MKS).

All chemicals were thoroughly degassed prior to use. $PhSiH_3$ (Aldrich, 99%), CD_3OD (CIL, 99.8 atom %), MeOH (Merck, >99.8%), and Ar (BOC, >99.99%) were used as supplied. H_2O was obtained from the in-house deionized water plant.

3. Experimental Results

Our previous work on the SiH_2/Me_2O system has suggested that the high-pressure limit for this reaction is reached at very high pressures ($>10^5$ Torr).[14,15] To facilitate accurate extrapolation to the high-pressure limit it is desirable to undertake the kinetic measurements up to as high a total pressure as possible. It is expected that the systems studied here will show similar pressure dependence to that exhibited for Me_2O. Consequently, the SiH_2/CD_3OD and SiH_2/MeOH experiments were performed up to 800 Torr, which is essentially the highest pressure attainable with the present apparatus. The SiH_2/H_2O reaction was studied up to 200 Torr, the maximum pressure for which reliable data could be obtained for this system because the signal levels decrease with increasing total pressure.

3.1. $SiH_2 + CD_3OD$, MeOH. The experimental observable is the SiH_2 relative concentration as a function of time following the photolysis laser pulse. A typical decay trace for MeOH, recorded at 294 K, is shown in Figure 1. Fits to such decay curves yield the pseudo-first-order rate constant, k_1, for the reaction.[24] A typical plot of k_1 versus reactant pressure (MeOH) at high total pressure is shown in Figure 2. Such plots give the second-order rate constant, k_2, at each total pressure. The MeOH and CD_3OD data were of similar quality. The CD_3OD data are the more extensive and are discussed first.

At the highest temperature studied, 423 K, the decay traces for CD_3OD do not fit to a single exponential. They exhibit both a fast and a slow component in the decay portion of the trace (see Figure 3). This is the same behavior observed for Me_2O.[15] It was demonstrated in that case that the behavior arises because of equilibrium being established between the reactants and a reaction complex. There is rapid initial decay of the SiH_2 concentration, but as more of the complex is formed, the rate of the reverse reaction increases and SiH_2 reforms through

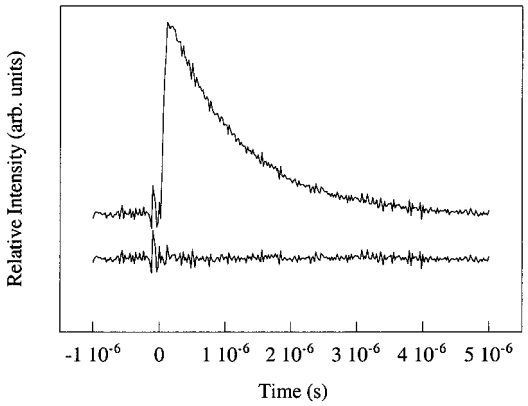

Figure 1. Typical average decay trace for SiH_2 (20 mTorr of $PhSiH_3$ precursor) reacting with 0.3 Torr CH_3OH at 700 Torr total pressure (Ar bath gas) and 294 K. The lower trace corresponds to the residuals from a biexponential fit.

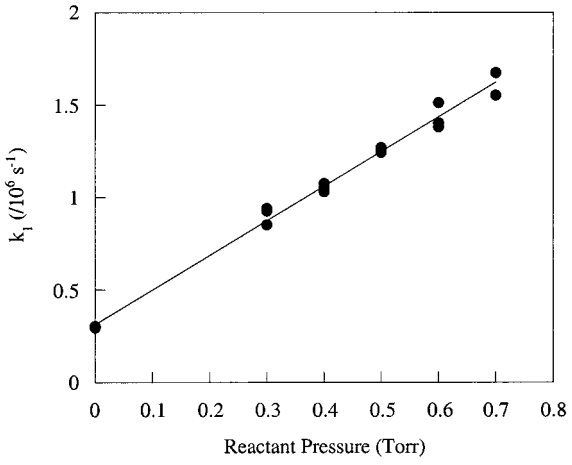

Figure 2. A typical plot of the pseudo-first-order rate constants versus reactant pressure for the reaction of SiH_2 with CH_3OH. The data were obtained at a total pressure of 700 Torr at 294 K in Ar bath gas.

dissociation of the complex. The SiH_2 concentration would decay to a plateau at the equilibrium SiH_2 concentration; however, another loss mechanism for SiH_2, such as reaction with another component of the mixture, diffusion from the observation region, or reaction of the complex to form products, will lead to further decay of the SiH_2 signal. This behavior is observed only at the highest temperature because the dissociation rate of the complex increases with increasing temperature. In the case of Me_2O, the slow component extended over a long time scale so that the decays essentially plateau, indicating that subsequent reaction of the complex is slow or not occurring. However, the slow component for the CD_3OD case decays quickly, as can be seen from Figure 3. This indicates that further reaction involving the complex is much more rapid in this case. These 423 K decay traces were fitted with an exponential rise and double exponential decay to model the fast and slow components.

Kinetic models for this type of reaction scheme predict a double exponential decay in the SiH_2 concentration.[7] If a preequilibrium between reactants and complex is approached, the sum of the fast and slow rate constants, k_{fast} and k_{slow}, in this decay is related to the bimolecular rate constant, k_2, via

$$k_{fast} + k_{slow} = k_2[CD_3OD] + c \qquad (1)$$

where c is a constant. From the fits to the data, k_{slow} is found to be both small compared with k_{fast} and approximately constant

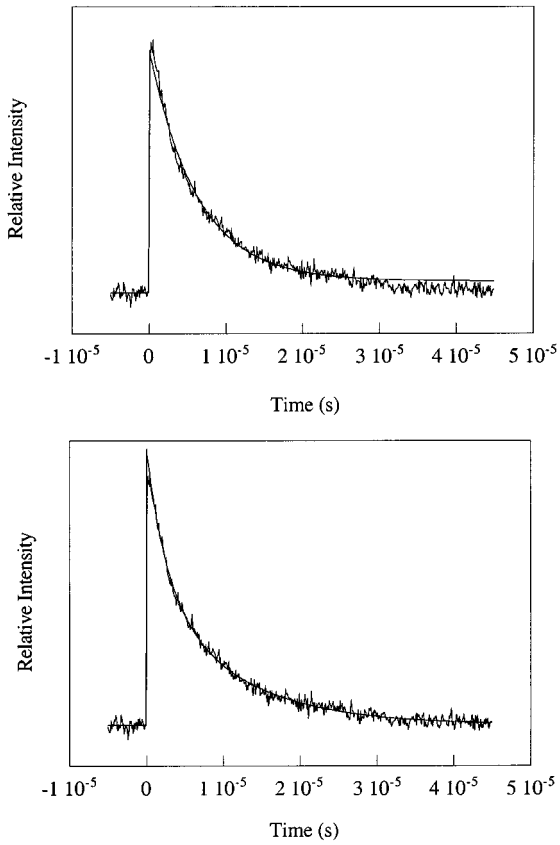

Figure 3. Typical average decay trace for SiH_2 (10 mTorr of $PhSiH_3$ precursor) reacting with 0.2 Torr CD_3OD at 500 Torr total pressure (Ar bath gas) and 423 K. The solid line in the upper plot is a fit to the data using a single-exponential decay with a variable offset. The solid line in the lower plot is the fit obtained using a double exponential decay. The double exponential decay is more accurate in its representation of the experimental trace than the single-exponential decay.

TABLE 1: A Summary of the k_2 Values Obtained in the Temperature Range 294−423 K for the SiH_2 Reaction with CD_3OD in Argon Bath Gas

total pressure (Torr)	k_2 (/10^{-11} cm^3 molecule^{-1} s^{-1})			
	294 K	334 K	375 K	423 K
100	2.56 ± 0.07	1.59 ± 0.04	1.18 ± 0.05	0.43 ± 0.02
200	4.48 ± 0.17	2.71 ± 0.06	1.95 ± 0.07	0.96 ± 0.06
300	5.45 ± 0.19	3.73 ± 0.09	2.47 ± 0.09	1.22 ± 0.11
350			2.95 ± 0.09	
400	6.57 ± 0.17		3.11 ± 0.10	1.51 ± 0.25
450		5.38 ± 0.20		
500	7.69 ± 0.15			2.18 ± 0.15
550		6.81 ± 0.16		
650	9.04 ± 0.20			
600			3.70 ± 0.35	2.12 ± 0.10
700	9.25 ± 0.50	7.05 ± 0.30	4.46 ± 0.28	
800		7.74 ± 0.25	4.94 ± 0.15	

with reactant concentration. Thus

$$k_{fast} \cong k_2[CD_3OD] + c' \qquad (2)$$

where $c' = c - k_{slow}$ is constant. A plot of k_{fast} versus $[CD_3OD]$ yields the second-order rate constant, k_2, from the slope.

The bimolecular rate constants for SiH_2 reacting with CD_3OD in Ar over the pressure range 100−800 Torr have been measured at four temperatures over the range 294−423 K. These rate constants are given in Table 1 and are plotted as a function of total pressure in Figure 4. The rate constants reported for 423 K are those extracted from the fast decay component of the overall decay trace, as discussed above. The rate constants

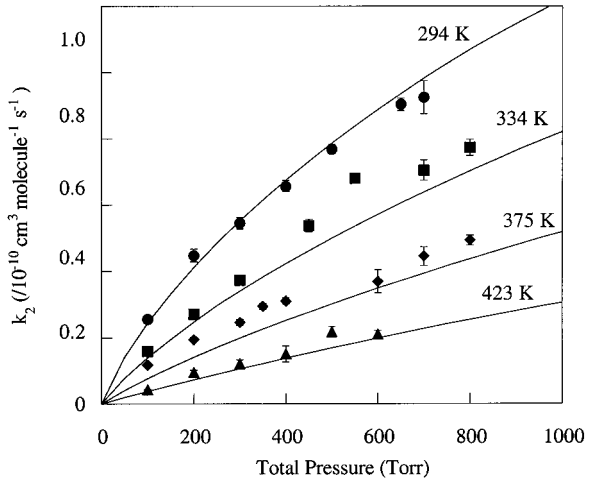

Figure 4. The pressure-dependent second-order rate constants for the SiH_2/CD_3OD reaction in Ar bath gas at 294 K (●), 334 K (■), 375 K (♦), and 423 K (▲) fitted with the RRKM/master equation analysis (solid lines).

decrease with increasing temperature and increase with increasing pressure.

It is convenient to extrapolate falloff data to the high-pressure limit using a Lindemann−Hinshelwood form, or a modified version thereof. However, such extrapolations are only reliable when the data are near the high-pressure limit. RRKM calculations for the $SiH_2 + Me_2O$ reaction, which is expected to show strong similarities to the $SiH_2 + CD_3OD$ reaction, have suggested that the high-pressure limit is several orders of magnitude above the highest experimental pressure of $\sim 10^3$ Torr.[14,15] Under these circumstances, simple Lindemann−Hinshelwood extrapolation of the data will not provide a meaningful estimate of k_2^∞. RRKM/master equation modeling has been used to obtain estimates of the high-pressure Arrhenius parameters (see section 4).

The negative temperature dependence seen in the data, that is, the reduction in the rate constant with increasing temperature, is typical of the behavior of systems involving the formation of an association complex.[29] This is additional evidence for the formation of such a complex for $SiH_2 + CD_3OD$.

As was demonstrated in the case of $SiH_2 + Me_2O$, the observation of biexponential decay enables the equilibrium constant at the corresponding temperature to be determined. The method has been given in detail previously.[15] Briefly, the biexponential decays are modeled based on the following reaction scheme, where R denotes the reactant:

$$SiH_2 + R \xrightarrow{k_f} SiH_2{-}R$$

$$SiH_2{-}R \xrightarrow{k_r} SiH_2 + R$$

$$SiH_2{-}R \xrightarrow{k_p} \text{products}$$

The reaction between SiH_2 and $PhSiH_3$ is not included as, because of the low concentration of $PhSiH_3$, its rate is much slower than that for the SiH_2/Me_2O reaction. k_p incorporates any process that removes the complex and, hence, SiH_2. The variation in SiH_2 concentration with time can be obtained by solution of the equations

$$\frac{d[SiH_2]_t}{dt} = -k_F[SiH_2]_t + k_r[SiH_2{-}R]_t \qquad (3)$$

$$\frac{d[SiH_2{-}R]_t}{dt} = k_F[SiH_2]_t - (k_r + k_p)[SiH_2{-}R]_t \qquad (4)$$

where $[X]_t$ is the concentration of species X at time t and $k_F = k_f[R]$, the t being omitted here because under pseudo-first-order conditions [R] is constant.

These equations can be solved analytically or by numerical integration and fitted to the experimental decay curves. We have chosen the latter approach as discussed in our previous publication, which also gives details of the numerical methods employed.[15] The fits yield values of k_F, k_r, and k_p. The k_F values are consistent with those determined from the biexponential analysis of the experimental data. The equilibrium constant, K_{eq}, is obtained from

$$K_{eq} = \frac{k_f}{k_r} = \frac{k_F/[CD_3OD]}{k_r} \qquad (5)$$

K_{eq} should be independent of the total pressure at which the experiment is performed and hence also of the bath gas used.[30] K_{eq} could only be determined at the highest pressures, so the pressure range over which it was measured was limited. The average value obtained for K_{eq} was $(2.15 \pm 0.70) \times 10^{-16}$ cm^3 molecule^{-1}.

The values for k_p were found to be high, typically only ~4 times lower than k_F. This reinforces the point made earlier that subsequent reaction involving the complex is rapid in this system. In the case of Me_2O, the process associated with k_p is slow, and we suggested that the slow decay of SiH_2 is associated with its diffusion from the volume interrogated by the laser or its reaction with other species or both rather than subsequent reaction of the complex. Because k_p for the present system is more than an order of magnitude larger than that for Me_2O, reaction rather than diffusion must be responsible.

Having a value for K_{eq} provides a means to obtain a direct experimental measurement of the critical energy, E_0. Because the reaction of interest involves a barrierless recombination, K_{eq} is related to E_0 via[30]

$$K_{eq} = \frac{Q_{AB}^{tr}}{Q_A^{tr}Q_B^{tr}} \frac{Q'_{AB}}{Q'_A Q'_B} \exp\left(\frac{E_0}{k_B T}\right) \qquad (6)$$

Here, Q_A^{tr}, Q_B^{tr}, and Q_{AB}^{tr} are the translational partition functions, while Q'_A, Q'_B, and Q'_{AB} are the product of the electronic, vibrational, and rotational partition functions. The value of K_{eq} thus depends exponentially on E_0. With the use of parameters determined from ab initio calculations (see section 4) to calculate the partition functions (ensuring that when incorporated into eq 6 the standard state is consistent with the concentration units used for K_{eq} and the recombination rate constant), an E_0 value consistent with the experimentally determined K_{eq} can be calculated. With this approach, we determine E_0 to be 83.0 ± 1.3 kJ mol^{-1}.

The results obtained for the reaction of SiH_2 with MeOH at 294 K are summarized in Table 2. A plot of the second-order rate constants versus total pressure is shown in Figure 5. This figure includes the corresponding data for CD_3OD for comparison. A comparison of the 294 K rate constants shows that those for CD_3OD are ~50% larger than the values for MeOH at 100 Torr, reducing to ~40% at 700 Torr.

3.2. $SiH_2 + H_2O$. A typical plot of pseudo-first-order rate constant versus reactant pressure is shown in Figure 6. A feature to note here is the *y*-axis scale. The pseudo-first-order rate constants are in the low 10^5 s^{-1} range, compared with the low

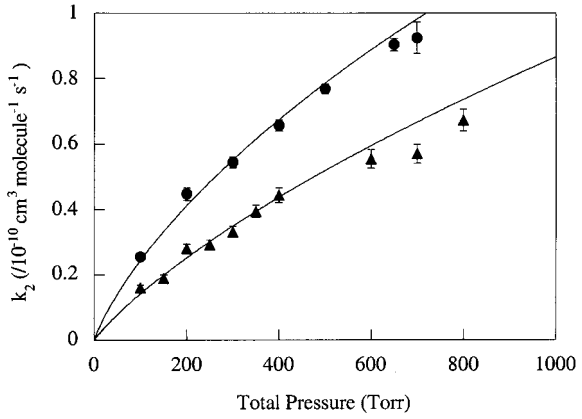

Figure 5. The pressure-dependent second-order rate constants for the SiH_2/CH_3OH reaction in Ar bath gas at 294 K (▲) fitted with the RRKM/master equation analysis (solid line). The rate constants for the SiH_2/CD_3OD reaction (●) and RRKM/master equation fit are shown for comparison.

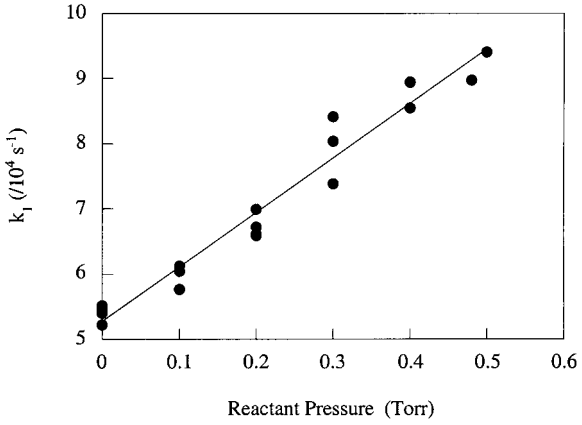

Figure 6. A typical plot of the pseudo-first-order rate constants versus reactant pressure for the reaction of SiH_2 with H_2O. The data were obtained at a total pressure of 200 Torr at 294 K in Ar bath gas.

TABLE 2: k_2 Values for the Reaction of SiH_2 with CH_3OH in Argon Bath Gas at 294 K

total pressure (Torr)	k_2 ($/10^{-11}$ cm^3 molecule^{-1} s^{-1})
100	1.60 ± 0.07
150	1.90 ± 0.07
200	2.80 ± 0.26
250	2.93 ± 0.10
300	3.31 ± 0.19
350	3.94 ± 0.22
400	4.44 ± 0.28
600	5.54 ± 0.11
700	5.70 ± 0.14
800	6.73 ± 0.30

TABLE 3: k_2 Values for the Reaction of SiH_2 with H_2O in Argon Bath Gas at 294 K

total pressure (Torr)	k_2 ($/10^{-12}$ cm^3 molecule^{-1} s^{-1})
50	0.67 ± 0.13
100	1.44 ± 0.18
150	1.99 ± 0.07
200	2.55 ± 0.13

10^6 s^{-1} range for similar data for CD_3OD (see Figure 4). This illustrates the slowing of the rate in moving to the H_2O system. The second-order rate constants are tabulated as a function of total pressure in Table 3. These data are plotted in Figure 7. Comparing the values for Me_2O, MeOH, and H_2O at the same pressure shows the dramatic reduction in the rate constant. At 200 Torr, the second-order rate constants for these three species,

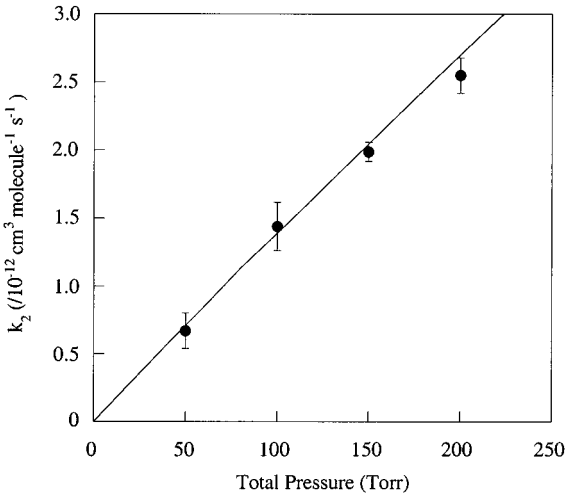

Figure 7. The pressure-dependent second-order rate constants for the SiH_2/H_2O reaction in Ar bath gas at 294 K (●) fitted with the RRKM/master equation analysis (solid line).

respectively, are $(9.7 \pm 0.3) \times 10^{-11}$, $(2.8 \pm 0.3) \times 10^{-11}$, and $(0.26 \pm 0.01) \times 10^{-11}$ cm^3 molecule^{-1} s^{-1}. Because the rate constants for D_2O are expected to be larger than those for H_2O, future experiments should focus on this species rather than H_2O.

4. Modeling

The pressure and temperature dependences of the rate constants have been modeled using an RRKM/master equation approach. This determines the rate constants for the association reactions from those for the unimolecular dissociation of the complex. Ab initio calculations, performed using the Gaussian suite of programs,[31] have been used to supply the necessary input data for the RRKM calculations. The ab initio calculations have been undertaken at a slightly lower level of theory than those recently reported by Heaven, Metha, and Buntine.[32] Their higher level calculations were necessitated by the desire to compare their SiH_2 calculations with GeH_2 calculations, and the latter required the higher level of theory. Our calculated energies are very similar to those reported by these authors. The calculations show that an association complex forms between SiH_2 and ROR′ species (R, R′ = CH_3, H). Heaven et al. have undertaken an extensive exploration of the reaction surface, in particular, examining the energy barriers to further reaction of the association complex. For the RRKM calculations, our primary interest is in using the ab initio calculations to determine the well depth and vibrational frequencies of the complex and the rotational constants at various Si−O bond separations. In the case of CD_3OD, we have an experimental determination of the dissociation energy with which to compare.

4.1. Ab Initio Calculations. The initial geometry of each complex and reactant was found using HF theory with a minimal basis set (HF/6-31G**) and then refined with increasing complexity of theory and basis set until the calculations were performed with the final theory/basis set, MP2/6-311+G**. Heaven et al. undertook their calculations at the MP2/6-311++G** level. The harmonic vibrational frequencies were scaled by the recommended factor of 0.9496 before use in the statistical mechanical calculation of thermodynamic quantities and the RRKM calculations.[33] No imaginary frequencies were found for any of the structures, indicating that they correspond to local minima on the relevant potential energy surfaces. A comparison of the scaled MP2/6-311+G** vibrational frequencies for SiH_2, CD_3OD, MeOH, and H_2O with experimental values shows that they lie within a few percent of each other.

The calculations show the electronic energy of the complexes to be stabilized by 89.1 and 68.1 kJ mol^{-1} compared with the reactants, methanol and water, respectively. In comparison, the electronic stabilization energy for the SiH_2-Me_2O complex was calculated to be 97.2 kJ mol^{-1}. Clearly, as H is replaced by Me, the complex stabilization energy is increased. The differences in zero-point energies, determined using scaled ab initio harmonic frequencies, are 75.4, 74.5, and 52.3 kJ mol^{-1} for CD_3OD, MeOH, and H_2O, respectively. The values for MeOH and H_2O are ~1 kJ mol^{-1} less than the corresponding values reported by Heaven et al. These authors did not report a value for CD_3OD. The value of 75.4 kJ mol^{-1} for CD_3OD is somewhat lower than the value of 83.0 ± 1.3 kJ mol^{-1} determined from the high-temperature equilibrium constant. An ab initio value lower than the experimental value was also found for the Me_2O-SiH_2 complex, although in that case the difference between them was less than is found for CD_3OD.[15]

4.2. RRKM/Master Equation Modeling. The SiH_2-ROR' fission and SiH_2/ROR' association reactions are described as

$$SiH_2 + ROR' \underset{k_2}{\overset{k_{-2}}{\rightleftharpoons}} SiH_2-ROR'$$

The bimolecular rate constant, k_2, is related to the unimolecular rate constant, k_{-2}, via the reaction equilibrium constant, $K_{eq} = k_2/k_{-2}$. RRKM/master equation calculations were carried out using the UNIMOL program suite[34] to obtain k_{-2} values for total pressures ranging over those covered experimentally and up to the high-pressure limit. K_{eq} is determined in the usual manner from the partition functions and enthalpy difference between reactants and products at 0 K[35] (see section 3.1). The bimolecular rate constant is then calculated from k_{-2} and K_{eq}.

The RRKM calculations are performed using the Gorin model, which has been extensively used for simple bond fission reactions producing fragments that do not show extensive electronic rearrangement (resonance stabilization). In this transition-state model, the stretch in the breaking bond is assigned as the reaction coordinate, the torsion around that bond becomes a free rotation, and the four bending modes that are destined to become external rotations of the products are weakened. The internal modes of this "loose" transition state are simply the vibrations and rotations of the independent product fragments, and the four low-frequency bending modes associated with the breaking bond are considered to be two two-dimensional internal rotations of the product fragments that are hindered by some angular potential function. The extent to which a fragment rotation in the transition state is hindered because of the presence of the other fragment is accounted for by reducing the moment of inertia of the free rotor to an "effective" moment of inertia for the hindered rotor as determined by the hindrance angle.

The input parameters for the RRKM/master equation calculations are based largely on the results of the ab initio calculations. Where there are multiple temperature data, the fitting parameters are well constrained. The variable parameters in our approach are $r^\dagger$, the Si−O bond length in the transition state, E_0, the critical energy, and the lowest frequency of the transition state. The Si−O bond stretch was selected as the reaction coordinate. The Si−O torsional motion was treated as a low-frequency vibration because treating it as a rotational motion leads to poor fits to the pressure-dependent data because the entropy is unacceptably high in the transition state. Two-dimensional rotors replaced the C−O−Si and/or H−O−Si bends and two H−Si−O bends associated with the breaking Si−O bond. Calculations using the alternate approach in which low-frequency rocking vibrations are used instead of two-dimensional rotations did not reproduce the experimental behavior. Consideration of steric hindrance between the fragments was not necessary in this model because of the lack of bulky fragments and the relatively long Si−O bond lengths. The external moment of inertia that corresponds to rotation about the Si−O axis was treated as active in both the molecule and the transition state. A vibrational assignment and the structural and thermodynamic properties for the complexes were obtained from the ab initio calculations.

In the master equation calculations, an exponential-down model for the energy transfer was employed:

$$P(E,E') = \frac{1}{N(E')} \exp\left[-\left(\frac{E'-E}{\alpha}\right)\right] \qquad (E < E') \quad (7)$$

where E' and E are the reactant energies before and after a collision, respectively, $N(E')$ is a normalizing factor, and α is a parameter related to the average downward energy transferred per collision, $\langle \Delta E_{down} \rangle$. The value for $\langle \Delta E_{down} \rangle$ is the only parameter varied in the master equation calculations. For Ar, Becerra et al.[36] found a constant value of 300 cm^{-1} applied over the range 298−665 K for the pressure dependence of SiH_2 reactions. This is consistent with values in the range 260−350 cm^{-1} at room temperature obtained from various kinetic and energy-transfer studies.[30] On the basis of these previous studies, we have used a $\langle \Delta E_{down} \rangle$ value for Ar of 320 cm^{-1}. We find that values in the range 300−350 cm^{-1} give similar results.

4.2.1. $SiH_2 + CD_3OD$. The Si−O bond was lengthened from a ground-state value of 0.238 nm to a transition-state value, $r^\dagger$ = 0.40−0.50 nm, depending on the temperature. The values used were 0.40, 0.43, 0.45, and 0.50 nm at temperatures of 423, 375, 334, and 294 K, respectively. The transition state becomes tighter as the temperature is increased. With $r^\dagger$ = 0.50 nm at 294 K, $A_{-2,\infty} = 10^{17.25}$ s^{-1}, a value within an acceptable range for simple fission reactions ($10^{16}-10^{17.5}$ s^{-1}).[30]

The molecular parameters used in the RRKM calculations are listed in Table 4. Figure 4 shows the calculated falloff curves with the experimental data, while Figure 8 shows the calculated curves extrapolated to the high-pressure limit. The calculated high-pressure behavior is very unusual and, not unexpectedly, reminiscent of the behavior calculated for the $SiH_2 + Me_2O$ reaction. The two systems have high-pressure limits predicted to occur at very high pressure, the temperature dependence is predicted to switch from negative to positive as the high-pressure limit is approached, and the rate constants are predicted to be extremely large at the high-pressure limit. The experimental data were obtained at pressures below 10^3 Torr, and the data are extrapolated to the high-pressure limit over several orders of magnitude. The high-pressure limit predictions are thus not expected to be necessarily accurate. For completeness, we note that the calculated k_2^∞ values are (0.92 ± 0.10) × 10^{-9}, (1.63 ± 0.45) × 10^{-9}, (1.95 ± 0.45) × 10^{-9}, and (2.47 ± 0.35) × 10^{-9} cm^3 molecule^{-1} s^{-1} at 294, 334, 375, and 423 K, respectively. An Arrhenius plot of the calculated values yields the following parameters: $\log(A/(\text{cm}^3\ \text{molecule}^{-1}\ \text{s}^{-1})) = -7.6 \pm 0.2$ and $E_a = 7.7 \pm 0.6$ kJ mol^{-1}.

It is important to note that even with a reasonably extensive data set one does not obtain a unique set of parameters from the RRKM/master equation fits. For example, changes in the E_0 value of ±1 kJ mol^{-1} could, with compensating changes in the other parameters, provide fits of similar quality to those shown in Figure 4. The E_0 determined from the RRKM/master equation analysis (83.7 kJ mol^{-1}) is consistent with the value determined from analysis of the 423 K data (83.0 ± 1.3 kJ mol^{-1}). The ab initio value is 75.4 kJ mol^{-1}.

TABLE 4: RRKM Parameters for the Decomposition of the SiH_2-CD_3OD Complex

	reactant	transition state
frequencies (cm^{-1})	2681	2707
	2283	2247
	2258	2203
	2108	2082
	2020	2049
	1982	2044
	1090	1122
	1047	1052
	1037	1043
	1026	1021
	982	1014
	935	960
	883	877
	808	749
	720	215
	682	200
	365	
	309	
	191	
	163	
	113	
rotational constants (cm^{-1})[a]		
inactive external	0.130 (1, 2)	0.033 (1, 2)
active external	0.730 (1, 1)	0.644 (1, 1)
internal		
SiH_2		7.602 (1, 2)[b]
CD_3OD		0.608 (1, 2)[b]
$\log(A_\infty/s^{-1})$ at 294 K		17.25
path degeneracy		1.0
critical energy, E_0 (kJ mol^{-1})		83.7
Lennard-Jones parameters	σ_{LJ}, ϵ_{LJ}	3.7, 172 (Ar bath gas)

[a] Quantities in parentheses are symmetry number and dimension, respectively. [b] Rotational constants for $r^\dagger = 0.50$ nm.

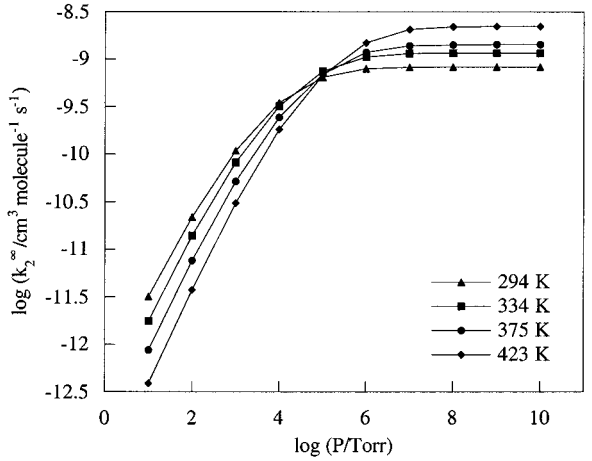

Figure 8. A plot of the pressure dependence of the rate constants for the SiH_2/CD_3OD reaction calculated from the RRKM/master equation fit to the data shown in Figure 5.

4.2.2. SiH_2 + MeOH. The RRKM parameters for MeOH can be determined by adjustment of the CD_3OD parameters to account for the changes upon the substitution of H for D. The principal changes are to the critical energy, arising because the change in vibrational frequencies leads to a change in the zero-point energy, the vibrational frequencies, and the rotational constants. The MeOH data therefore provide a further test for the parameters derived for CD_3OD.

The differences in zero-point energies between the association complex and reactants (SiH_2 and MeOH or CD_3OD) are 75.4 and 74.5 kJ mol^{-1} for the deuterated and nondeuterated species, respectively, giving a 0.9 kJ mol^{-1} difference between MeOH and CD_3OD. This does not, however, provide a complete estimate of the effect of deuteration on E_0 because the association complex and transition state have more vibrational frequencies than the products: some vibrations of the complex become rotational and translational degrees of freedom of the separated products. To get an improved estimate for the effect of deuteration on E_0, ab initio calculations have been performed on the association complex with an increasing Si−O bond length. Ideally, the calculations at equilibrium and transition-state Si−O bond length should be compared. Unfortunately, the calculations did not work at the 294 K transition-state extension of 0.50 nm; however, they work from the equilibrium Si−O bond length of 0.2038 nm out to a Si−O bond extension of 0.40 nm. Extrapolating the frequency changes observed from equilibrium to 0.4 nm leads to an estimate of a change in E_0 of 1.7 kJ mol^{-1} between CD_3OD and MeOH.

TABLE 5: RRKM Parameters for the Decomposition of the SiH_2-MeOH Complex

	reactant	transition state
frequencies (cm^{-1})	3678	3715
	3074	3031
	3039	2968
	2943	2902
	2020	2049
	1981	2044
	1447	1456
	1438	1441
	1442	1433
	1312	1312
	1140	1136
	1066	1042
	980	1022
	976	1014
	755	303
	697	200
	493	
	322	
	211	
	180	
	142	
rotational constants (cm^{-1})[a]		
inactive external	0.149 (1, 2)	0.036 (1, 2)
active external	0.980 (1, 1)	0.845 (1, 1)
internal		
SiH_2		7.602 (1, 2)[b]
CH_3OH		0.618 (1, 2)[b]
$\log(A_\infty/s^{-1})$ at 294 K		17.25
path degeneracy		1.0
critical energy, E_0 (kJ mol^{-1})		82.0
Lennard-Jones parameters	σ_{LJ}, ϵ_{LJ}	3.7, 172 (Ar bath gas)

[a] Quantities in parentheses are symmetry number and dimension, respectively. [b] Rotational constants for $r^\dagger = 0.50$ nm.

The RRKM/master equation prediction for MeOH with E_0 reduced by 1.7 kJ mol^{-1} is compared with the data in Figure 5. The RRKM parameters are listed in Table 5. It can be seen that the prediction and the data match very well, indicating the predictive power of the RRKM/master equation parameters. The value of k_2^∞ is calculated to be 1.43×10^{-9} cm^3 molecule^{-1} s^{-1} at 294 K.

4.2.3. SiH_2 + H_2O. The H_2O data are less extensive than those for the methanol system. There are too few data to determine a well-constrained set of RRKM parameters for this system. However, given that this system is expected to show strong similarities to the MeOH, CD_3OD, and Me_2O systems, a reasonable set of parameters can be determined.

The RRKM/master equation fit to the H_2O data is shown in Figure 7. The RRKM parameters are listed in Table 6. The fit

TABLE 6: RRKM Parameters for the Decomposition of the SiH_2-H_2O Complex

	reactant	transition state
frequencies (cm^{-1})	3764	3802
	3654	3689
	2035	2049
	1998	2044
	1558	1547
	988	1014
	787	200
	661	
	500	
	396	
	279	
	170	
rotational constants (cm^{-1})[a]		
inactive external	0.307 (1, 2)	0.058 (1, 2)
active external	2.849 (1, 1)	2.847 (1, 1)
internal		
SiH_2		7.602 (1, 2)[b]
H_2O		11.567 (2, 2)[b]
$\log(A_\infty/s^{-1})$ at 294 K		16.6
path degeneracy		1.0
critical energy, E_0 (kJ mol^{-1})		64.9
Lennard-Jones parameters	σ_{LJ}, ϵ_{LJ}	3.45, 196 (Ar bath gas)

[a] Quantities in parentheses are symmetry number and dimension, respectively. [b] Rotational constants for $r^\dagger = 0.50$ nm.

was obtained with an E_0 of 64.9 kJ mol^{-1}, compared with the ab initio value of 52.3 kJ mol^{-1}. The value of k_2^∞ is calculated to be 1.3×10^{-9} cm^3 $molecule^{-1}$ s^{-1} at 294 K.

5. Discussion

Evidence concerning the mechanism for SiH_2 reactions with ROR′-type molecules (R, R′ = H, CH_3) can be found in results from both solution and gas-phase studies of substituted silylenes reacting with ROR′ molecules (R, R′ = H, CH_3, CH_2CH_3) and from the results of ab initio studies. Competitive rate studies of dimethyl silylene, $SiMe_2$, and methylphenyl silylene, SiMePh, reacting with alcohols in solution have led to the proposal of a reaction mechanism in which these silylenes reversibly form an addition complex with the alcohol prior to an irreversible reaction to form products:[37]

$$SiR''_2 + ROR' \rightleftarrows R''_2Si-ORR' \rightarrow R''_2RSi-OR'$$

where R, R′, R″ = H or an alkyl group.

This mechanism has been reinforced in observations of gas-phase $SiMe_2$ reactions with CH_3OH/CH_3OD and CH_3OCH_3 by Baggott et al.[8] Importantly, when R = R′ = CH_3, the irreversible reaction of the complex to form products appears not to occur because products are not detected.[8] Our experiments on the SiH_2-Me_2O system are consistent with this.

Ab initio calculations show that rearrangement of the SiH_2-Me_2O complex involves a high-energy barrier (193.3 kJ mol^{-1} [32]). However, when R and/or R′ are H, the barrier is much lower because a H shift requires much less energy than a methyl migration. For H_2O, three reaction channels for the SiH_2-H_2O complex have been identified, one leading to silanol and the others to *syn*- and *anti*-hydroxysilene + H_2. The barriers are calculated to all be very similar, lying 37−39 kJ mol^{-1} above $SiH_2 + H_2O$. For SiH_2 + MeOH, the corresponding three channels are calculated to be present, again with barriers that are very similar. In this case, the barrier is quite low, being calculated to lie in the range 13−16 kJ mol^{-1} for the three channels.

The negative temperature dependence seen for $SiH_2 + CD_3OD$ and the total pressure dependence of the rate constants for all of the reactants are indications of a mechanism involving complex formation. Particularly important is the observation for CD_3OD of biexponential decays at elevated temperatures (423 K) because this is direct evidence for complex formation and subsequent decay. These CD_3OD decays also provide evidence that there is rapid loss of the complex in this system, unlike the case for Me_2O. The low barriers calculated for reaction of the SiH_2-MeOH complex raise the possibility that the rapid loss of the complex is associated with it undergoing further reaction.

The well depth determined from the RRKM/master equation fits to the data for CD_3OD is 83.7 kJ mol^{-1}, compared with 75.4 kJ mol^{-1} determined by ab initio calculations. This is a larger difference than was found for the Me_2O case for which the relevant values are 87 and 84.3 kJ mol^{-1}, respectively. While the H_2O data are very poorly constrained, we note that the E_0 used for those calculations was also significantly higher than the ab initio value (64.9 vs 52.3 kJ mol^{-1}). The evidence, while far from compelling, hints at the ab initio calculations becoming increasingly in error as H replaces methyl in these systems.

As was the case for the Me_2O system, the high-pressure limit values for the rate constants as determined by the RRKM/master equation calculations are highly unusual. An issue with the analysis is the large pressure range over which the data are extrapolated to the high-pressure limit. Falloff curves approach the high-pressure limit slowly. For this reason, rather than quote high-pressure limit values, we note the pressure values for which k_2 is 90% of k_2^∞. The value of k_2/k_2^∞ is predicted to be ∼0.9 at pressures in the 10^5-10^6 Torr range, depending on the temperature. Thus the extrapolation to the high-pressure region is over ∼2−3 orders of magnitude in pressure and, consequently, it is likely that the high-pressure rate constants and the high pressure required to reach this limit are not reliable. Nevertheless, it is interesting that the calculations for the present systems show the same unusual trends as seen in the Me_2O calculations. Specifically, the high-pressure limit is reached at unusually high pressure, the reaction is very efficient, with indications that the high-pressure limit rate constant is larger than the Lennard-Jones collision rate constant, and in the high-pressure limit, the reaction is predicted to have a positive temperature dependence, indicating a barrier to reaction.

These unusual predictions for the SiH_2-Me_2O system were attributed to the shallow well depth for the complex, coupled with the large Si−O bond length at the transition state. The SiH_2-MeOH and SiH_2-H_2O systems have similar attributes in these respects to the SiH_2-Me_2O system, so it is not unexpected that the predictions will be similar.

The arguments put forward for the SiH_2-Me_2O case also apply to the systems studied here and can be summarized as follows. With respect to the high pressure required for the high-pressure limit, the larger the microscopic rate constants for dissociation are, the higher the pressure required to reach the high-pressure limit is because the collisional energy-transfer rate constants must exceed the dissociation rate constants at the high-pressure limit. The microscopic rate constants, $k(E)$, are given by RRKM theory as[30]

$$k(E) = \frac{\int_0^{E-E_0} \rho^\dagger(E_+)\, dE_+}{h\rho(E)} \qquad (8)$$

Here $\rho^\dagger(E_+)$ is the density of states of the transition state at energy E_+ above the critical energy E_0, $\rho(E)$ is the density of states of the molecular reactant and h is Planck's constant. The

very low critical energy for dissociation means that the denominator in this expression will be much smaller than usual and the $k(E)$ values will be unusually large. For this reason, large high-pressure-limit pressures will be a general feature of systems with unusually low E_0 values. This argument was supported using comparisons with other systems, including those with large E_0 and those with unusually low E_0.

A high efficiency for the reaction implies that it involves a long-range attraction between the reactant species, and this is consistent with the large Si−O bond length in the transition state. The positive temperature dependence in the high-pressure limit can be rationalized by the relative magnitudes of the intermolecular potential at the transition state and the "centrifugal potential" barrier associated with the orbital angular momentum of the approaching reactants. A weak bond coupled with a transition state at large separation means that the potential energy is not much reduced from the asymptotic value at the transition state. The centrifugal term can become important by creating a barrier at low temperatures, leading to a positive temperature dependence in this temperature regime.

Acknowledgment. This work was supported in part by the Australian Research Council. U.N.A. acknowledges the financial support provided by an Australian Postgraduate Award. The help of the Mechanical, Glassblowing and Engineering Workshop staff at Flinders University is gratefully acknowledged. We thank Professor Robin Walsh for helpful correspondence.

References and Notes

(1) Jasinski, J. M.; Meyerson, B. S.; Scott, B. A. *Annu. Rev. Phys. Chem*. **1987**, *38*, 109.
(2) Gaspar, P. P. In *Reactive Intermediates*; Jones, M., Jr., Moss, R. A., Eds.; Wiley: New York, 1978; Vol. 1, p 229.
(3) Gaspar, P. P. In *Reactive Intermediates*; Jones, M., Jr., Moss, R. A., Eds.; Wiley: New York, 1981; Vol. 2, p 335.
(4) Gaspar, P. P. In *Reactive Intermediates*; Jones, M., Jr., Moss, R. A., Eds.; Wiley: New York, 1985; Vol. 3, p 333.
(5) Inoue, G., Suzuki, M. *Chem. Phys. Lett*. **1985**, *122*, 361.
(6) Baggott, J. E.; Blitz, M. A.; Frey, H. M.; Lightfoot, P. D.; Walsh, R. *Chem. Phys. Lett*. **1987**, *135*, 39.
(7) Baggott, J. E.; Blitz, M. A.; Lightfoot, P. D. *Chem. Phys. Lett*. **1989**, *154*, 330.
(8) Baggott, J. E.; Blitz, M. A.; Frey, H. M.; Lightfoot, P. D.; Walsh, R. *Int. J. Chem. Kinet*. **1992**, *24*, 127.
(9) Jasinski, J. M.; Becerra, R.; Walsh, R. *Chem. Rev*. **1995**, *95*, 1203.
(10) Becerra, R.; Walsh, R. In *Research in Chemical Kinetics*; Compton, R. G., Hancock, G., Eds.; Elsevier Science: Amsterdam, 1995; Vol. 3.
(11) Al-Rubaiey, N.; Walsh, R. *J. Phys. Chem.* **1994**, *98*, 5303.
(12) Becerra, R.; Walsh, R. *Int. J. Chem. Kinet*. **1994**, *26*, 45.
(13) Becerra, R.; Cannady, J. P.; Walsh, R. *J. Phys. Chem. A* **1999**, *103*, 4457.
(14) Becerra, R.; Carpenter, I. W.; Gutsche, G. J.; King, K. D.; Lawrance, W. D.; Staker, W. S.; Walsh, R. *Chem. Phys. Lett*. **2001**, *333*, 83.
(15) Alexander, U. N.; King, K. D.; Lawrance, W. D. *Phys. Chem. Chem. Phys.* **2001**, *3*, 3085.
(16) Raghavachari, K.; Chandrasekhar, J.; Gordon, M. S.; Dykema, K. J. *J. Am. Chem. Soc.* **1984**, *106*, 5853.
(17) Su, S.; Gordon, M. S. *Chem. Phys. Lett.* **1993**, *204*, 306.
(18) Staker, W. S.; King, K. D.; Gutsche, G. J.; Lawrance, W. D. *J. Chem. Soc., Faraday Trans*. **1991**, *87*, 2421.
(19) Staker, W. S.; King, K. D.; Gutsche, G. J.; Lawrance, W. D. *J. Chem. Soc., Faraday Trans*. **1992**, *88*, 659.
(20) Hayes, F. J.; Gutsche, G. J.; Lawrance, W. D.; Staker, W. S.; King, K. D. *Combust. Flame* **1995**, *100*, 653.
(21) Hayes, F. J.; Lawrance, W. D.; Staker, W. S.; King, K. D. *J. Phys. Chem*. **1996**, *100*, 11314.
(22) Hayes, F. J.; Lawrance, W. D.; Staker, W. S.; King, K. D. *Chem. Phys. Lett.* **1994**, *231*, 530.
(23) Buntine, M. A.; Gutsche, G. J.; Staker, W. S.; Heaven, M. W.; King, K. D.; Lawrance, W. D. *Z. Phys. Chem.*, in press.
(24) Alexander, U. N.; Trout, N. A.; King, K. D.; Lawrance, W. D. *Chem. Phys. Lett*. **1999**, *299*, 291.
(25) Alexander, U. N.; King, K. D.; Lawrance, W. D. *Chem. Phys. Lett*. **2000**, *319*, 529.
(26) Jasinski, J. M.; Chu, J. O. *J. Chem. Phys.* **1988**, *88*, 1678.
(27) Ishikawa, H.; Kajimoto, O. *J. Phys. Chem*. **1994**, *98*, 122.
(28) Chu, J. O.; Beach, D. B.; Jasinski, J. M. *J. Phys. Chem*. **1987**, *91*, 5340.
(29) Troe, J. *J. Chem. Soc., Faraday Trans*. **1994**, *90*, 2303.
(30) Gilbert, R. G.; Smith, S. C. *Theory of Unimolecular and Recombination Reactions*; Blackwell Scientific Publications: Oxford, U.K., 1990.
(31) Frisch, M. J.; Trucks, G. W.; Schlegel, H. B.; Scuseria, G. E.; Robb, M. A.; Cheeseman, J. R.; Zakrzewski, V. G.; Montgomery, J. A., Jr.; Stratmann, R. E.; Burant, J. C.; Dapprich, S.; Millam, J. M.; Daniels, A. D.; Kudin, K. N.; Strain, M. C.; Farkas, O.; Tomasi, J.; Barone, V.; Cossi, M.; Cammi, R.; Mennucci, B.; Pomelli, C.; Adamo, C.; Clifford, S.; Ochterski, J.; Petersson, G. A.; Ayala, P. Y.; Cui, Q.; Morokuma, K.; Malick, D. K.; Rabuck, A. D.; Raghavachari, K.; Foresman, J. B.; Cioslowski, J.; Ortiz, J. V.; Stefanov, B. B.; Liu, G.; Liashenko, A.; Piskorz, P.; Komaromi, I.; Gomperts, R.; Martin, R. L.; Fox, D. J.; Keith, T.; Al-Laham, M. A.; Peng, C. Y.; Nanayakkara, A.; Gonzalez, C.; Challacombe, M.; Gill, P. M. W.; Johnson, B. G.; Chen, W.; Wong, M. W.; Andres, J. L.; Head-Gordon, M.; Replogle, E. S.; Pople, J. A. *Gaussian 98*, revision A.7; Gaussian, Inc.: Pittsburgh, PA, 1998.
(32) Heaven, M. W.; Metha, G. F.; Buntine, M. A. *J. Phys. Chem. A* **2001**, *105*, 1185.
(33) Scott, A. P.; Radom, L. *J. Phys. Chem*. **1996**, *100*, 16505.
(34) Gilbert, R. G.; Smith, S. C.; Jordan, M. J. T. *UNIMOL program suite (calculation of falloff curves for unimolecular and recombination reactions)*; Sydney University: Sydney, Australia, 1993.
(35) Benson, S. W. *Thermochemical Kinetics: Methods for Estimation of Thermochemical Data and Rate Parameters*; Wiley and Sons: New York, 1968.
(36) Becerra, R.; Frey, H. M.; Mason, B. P.; Walsh, R.; Gordon, M. S. *J. Chem. Soc., Faraday Trans.* **1995**, *91*, 2723.
(37) Steele, K. P.; Weber, W. P. *Inorg. Chem.* **1981**, *20*, 1302.